Siberian Branch of Russian Academy of Science
BUDKER INSTITUTE OF NUCLEAR PHYSICS

R.N. Lee, A.I. Milstein, V.M. Strakhovenko

# LARGE COULOMB CORRECTIONS IN HIGH-ENERGY PHOTON SPLITTING

Budker INP 97-85

Novosibirsk
1997

# Large Coulomb corrections in high-energy photon splitting

*R.N. Lee, A.I. Milstein, V.M. Strakhovenko*

Budker Institute of Nuclear Physics SB RAS
630090 Novosibirsk, Russia

**Abstract**

The Coulomb corrections to the helicity amplitudes of high-energy photon splitting are examined. The consideration is based on the amplitudes obtained exactly in the parameter $Z\alpha$ within the quasiclassical approach valid for small angles between all photon momenta. We consider the case when the transverse momenta of both final photons are much larger than the electron mass. It is shown that at $Z\alpha \sim 1$ the Coulomb corrections essentially change the result for the cross section as compared to the Born approximation. The effect of screening is also taken into account.

# 1 Introduction

One of the most interesting nonlinear QED processes at high energy is splitting of one photon into two in electric fields of atoms. The total cross section of this process does not decrease with increasing photon energy. First results on the observation of high-energy photon splitting on atoms have been obtained recently in the Budker Institute of Nuclear Physics [1]. Theoretically this process has been investigated in [2, 3, 4, 5, 6] only in the lowest order in $Z\alpha$ (Born approximation), $Z|e|$ is the nucleus charge, $\alpha = e^2/4\pi = 1/137$ is the fine-structure constant, $e$ is the electron charge. Though the expressions obtained in [2, 3] are rather cumbersome, some numerical calculations based on the results of these papers have been carried out in [5, 6] . Using the Weizsäcker-Williams method providing the logarithmic accuracy the cross section of the process has been obtained in an essentially simpler form in [4]. The comparison of the exact cross section [5] with the approximate result [4] has shown that the accuracy is better than 20%. The Coulomb corrections to the cross section, which can essentially modify the result as compared to that obtained in the Born approximation, have been unknown up to now.

Recently we derived in [7] the analytical expressions for the high-energy photon-splitting amplitudes. The result was obtained exactly in the parameter $Z\alpha$ at small angles $f_2$ and $f_3$ between the momenta $\mathbf{k}_2$, $\mathbf{k}_3$ of the final photons and the momentum $\mathbf{k}_1$ of the initial one. This region of angles gives the main contribution to the total cross section of the process. Small angles and high energies of photons allow one to use the quasiclassical approach developed in [8, 9] at the investigation of coherent photon scattering in a Coulomb field (Delbrück scattering). This approach gives the transparent picture of the phenomenon and essentially simplifies the calculation.

In the present paper we start from the analitycal results obtained in [7] and investigate the role of the Coulomb corrections in the photon splitting process. We restrict ourselves to the case $|\mathbf{k}_{2\perp}| = \omega_2 f_2 \gg m$, $|\mathbf{k}_{3\perp}| = \omega_3 f_3 \gg m$ ( $\omega_i = |\mathbf{k}_i|$, $m$ is the electron mass) when the amplitudes can be essentially simplified. A pure Coulomb potential as well as the influence of screening is considered.

## 2 Kinematics of the process

Below we use the coordinate system with $z$-axis directed along $\mathbf{k}_1$ so that $a_z = \mathbf{a}\mathbf{k}_1/\omega_1$ and $\mathbf{a}_\perp = \mathbf{a} - a_z\mathbf{k}_1/\omega_1$ for an arbitrary vector $\mathbf{a}$. According to the uncertainty relation the lifetime of the virtual electron-positron pair is $\tau \sim \omega_1/(m^2 + \tilde{\Delta}^2)$, where $\tilde{\Delta} = \max(|\mathbf{k}_{2\perp}|, |\mathbf{k}_{3\perp}|) \ll \omega_1$. The characteristic transverse distance between the virtual particles can be estimated as $(m^2 + \tilde{\Delta}^2)^{-1/2}$, which is much smaller than the length of the electron-positron loop. The characteristic impact parameter is $\varrho \sim 1/\Delta$ , where $\mathbf{\Delta} = \mathbf{k}_2 + \mathbf{k}_3 - \mathbf{k}_1$ is the momentum transfer. At small $\mathbf{k}_{2\perp}$ and $\mathbf{k}_{3\perp}$ ($f_{2,3} \ll 1$) we have

$$\mathbf{\Delta}^2 = (\mathbf{k}_{2\perp} + \mathbf{k}_{3\perp})^2 + \frac{1}{4}\left(\frac{\mathbf{k}_{2\perp}^{\,2}}{\omega_2} + \frac{\mathbf{k}_{3\perp}^{\,2}}{\omega_3}\right)^2 . \qquad (1)$$

The characteristic angular momentum is $l \sim \omega/\Delta \gg 1$ , and the quasiclassical approximation can be applied.

Let us discuss a screened Coulomb potential. In the Thomas-Fermi model the screening radius is $r_c \sim (m\alpha)^{-1}Z^{-1/3}$ . If $R \ll 1/\Delta \ll r_c$ ($R$ is the nucleus radius), then the screening is inessential and the amplitude coincides with that in the pure Coulomb field. At $1/\Delta \sim r_c$ the screening should be taken into account. Obviously, the impact parameters $\varrho \gg r_c$ do not contribute to the total cross section. Due to this fact we shall concentrate ourselves on the momentum transfer region corresponding to the impact parameter $\varrho \leq r_c$. If $\mathbf{k}_{2\perp}^{\,2}/\omega_2 + \mathbf{k}_{3\perp}^{\,2}/\omega_3 \ll r_c^{-1}$ , then it follows from (1) that the condition $\varrho \leq r_c$ holds only when $|\mathbf{\Delta}_\perp| = |\mathbf{k}_{2\perp} + \mathbf{k}_{3\perp}| \geq r_c^{-1}$. Thus, the main contribution to the amplitude is given by the region of momentum transfer $\mathbf{\Delta}_\perp$, restricted from below.

According to the Furry theorem the photon-splitting amplitude is an odd function with respect to the parameter $Z\alpha$. In the Born approximation the amplitude is proportional to the Fourier transform of the Coulomb potential ($\sim Z\alpha/\Delta^2$). Therefore, the region of very small momentum transfers $\Delta \sim r_c^{-1}$ is essential, and screening should be taken into account. In next orders of perturbation theory with respect to the parameter $Z\alpha$ ( Coulomb corrections ) the integral over all momenta corresponding to the external field should be taken provided that their sum is equal to $\mathbf{\Delta}$. Therefore, even at $\Delta \sim r_c^{-1}$ each momentum is not small and the screening can be neglected. In the Born approximation the screening can be taken into account by multiplying the amplitude by the factor $[1 - F(\Delta^2)]$, where $F(\Delta^2)$ is the atomic electron form factor. Thus, to find the photon-splitting amplitude in a screened Coulomb field it is sufficient to solve the problem in a pure Coulomb field.

## 3 Amplitudes

It is convenient to perform the calculations in terms of the helicity amplitudes $M_{\lambda_1\lambda_2\lambda_3}(\mathbf{k}_1, \mathbf{k}_2, \mathbf{k}_3)$. The longitudinal components of the polarization vectors $\mathbf{e}_i$ can be eliminated owing to the relation $\mathbf{e}_i\mathbf{k}_i = 0$ which leads to $e_z = -\mathbf{e}_\perp\mathbf{k}_\perp/\omega$. After that within a small-angle approximation one can neglect the difference between vectors $(\mathbf{e}_{2,3})_\perp$ and the polarization vectors of photons propagating along $\mathbf{k}_1$ and having the same helicities.

Therefore, the amplitudes $M_{\lambda_1\lambda_2\lambda_3}(\mathbf{k}_1,\mathbf{k}_2,\mathbf{k}_3)$ are expressed in terms of the polarization vectors $\mathbf{e}$ and $\mathbf{e}^*$ corresponding to positive and negative helicities, respectively. It is sufficient to calculate three amplitudes, for instance, $M_{+--}(\mathbf{k}_1,\mathbf{k}_2,\mathbf{k}_3)$ , $M_{+++}(\mathbf{k}_1,\mathbf{k}_2,\mathbf{k}_3)$ and $M_{++-}(\mathbf{k}_1,\mathbf{k}_2,\mathbf{k}_3)$ . The rest amplitudes can be obtained by substitutions:

$$M_{+-+}(\mathbf{k}_1,\mathbf{k}_2,\mathbf{k}_3) = M_{++-}(\mathbf{k}_1,\mathbf{k}_3,\mathbf{k}_2)\,,$$
$$M_{-\lambda_2\lambda_3}(\mathbf{k}_1,\mathbf{k}_2,\mathbf{k}_3) = M_{+\Lambda_2\Lambda_3}(\mathbf{k}_1,\mathbf{k}_2,\mathbf{k}_3)\,(\mathbf{e}\leftrightarrow\mathbf{e}^*)\,,$$

where $\Lambda$ denotes the helicity opposite to $\lambda$ Let us introduce two-dimensional vectors $\mathbf{f}_2 = \mathbf{k}_{2\perp}/\omega_2$, $\mathbf{f}_3 = \mathbf{k}_{3\perp}/\omega_3$ ($|\mathbf{f}_{2,3}| \ll 1$) and $\mathbf{f}_{23} = \mathbf{f}_2 - \mathbf{f}_3$. We represent the amplitudes obtained in [7] for $|\mathbf{k}_{2\perp}| \gg m$, $|\mathbf{k}_{3\perp}| \gg m$ in the following form

$$M = \frac{8e^3}{\pi^2\omega_1\omega_2\omega_3\boldsymbol{\Delta}^2}\int d\mathbf{q}\,(\mathbf{T}\boldsymbol{\nabla}_\mathbf{q})\,\mathrm{Im}\left(\frac{|\mathbf{q}+\boldsymbol{\Delta}|}{|\mathbf{q}-\boldsymbol{\Delta}|}\right)^{2iZ\alpha} \quad ; \tag{2}$$

$$\mathbf{T}_{+--} = \mathbf{e}\int_0^{\omega_2} d\varepsilon\,\frac{\kappa_2\,(\mathbf{e}^*,\kappa_2\mathbf{f}_2-\boldsymbol{\Delta})}{4(\mathbf{e}^*\mathbf{f}_3)(\mathbf{e}^*\mathbf{f}_{23})(\mathbf{e}^*\mathbf{a})} + \begin{pmatrix}\omega_2\leftrightarrow\omega_3\\ \mathbf{f}_2\leftrightarrow\mathbf{f}_3\end{pmatrix} \quad ;$$

$$\mathbf{T}_{+++} = \mathbf{e}^*\int_0^{\omega_2} d\varepsilon\left[\frac{\omega_3\varepsilon\kappa_2}{\omega_2\mathcal{D}_3}\left(\frac{\omega_3}{2}+\frac{(\mathbf{e}^*\mathbf{f}_3)}{(\mathbf{e}^*\mathbf{a})}(\kappa_2^2+\kappa_3^2)\right)+\frac{(\kappa_2^2+\kappa_3^2)}{8(\mathbf{e}^*\mathbf{a})(\mathbf{e}\mathbf{f}_{23})}\right] + \begin{pmatrix}\omega_2\leftrightarrow\omega_3\\ \mathbf{f}_2\leftrightarrow\mathbf{f}_3\end{pmatrix};$$

$$\mathbf{T}_{++-} = \mathbf{e}\int_0^{\omega_2} d\varepsilon\left[\frac{\omega_3\kappa_2\kappa_3}{\omega_1\mathcal{D}_1}\left(\frac{\kappa_2-\varepsilon}{2}-\frac{(\mathbf{e}\mathbf{f}_{23})}{(\mathbf{e}\mathbf{a})}(\kappa_2^2+\varepsilon^2)\right)+\frac{(\kappa_2^2+\varepsilon^2)}{8(\mathbf{e}^*\mathbf{f}_3)(\mathbf{e}\mathbf{a})}\right]+$$

$$+\mathbf{e}\,\omega_2\int_{-\omega_3}^{0} d\varepsilon\,\kappa_3\left[\frac{\kappa_3(\kappa_2^2+\varepsilon^2)}{(\mathbf{e}^*\mathbf{b})}\left(\frac{(\mathbf{e}^*\mathbf{f}_{23})}{\omega_1\mathcal{D}_1}+\frac{(\mathbf{e}^*\mathbf{f}_2)}{\omega_3\mathcal{D}_2}\right)-\frac{\varepsilon\kappa_3+\kappa_2^2}{2\omega_1\mathcal{D}_1}+\frac{\varepsilon^2-\kappa_2\kappa_3}{2\omega_3\mathcal{D}_2}\right].$$

where $\mathbf{q}$ is a two-dimensional vector lying in the plane perpendicular to $\mathbf{k}_1$, $\boldsymbol{\Delta}$ denotes $\boldsymbol{\Delta}_\perp$.

In eq. (2) the following notation is used:

$$\kappa_2 = \omega_2 - \varepsilon\,,\ \kappa_3 = \omega_3 + \varepsilon\,,\ \mathcal{D}_1 = \frac{\omega_2\kappa_3\mathbf{a}^2 - \omega_3\kappa_2\mathbf{b}^2}{\omega_1\varepsilon} - i0\ , \tag{3}$$

$$\mathcal{D}_2 = \frac{\omega_2\kappa_3\tilde{\mathbf{c}}^2 - \omega_1\varepsilon\mathbf{b}^2}{\omega_3\kappa_2}\,,\mathcal{D}_3 = \frac{\omega_1\varepsilon\mathbf{a}^2+\omega_3\kappa_2\mathbf{c}^2}{\omega_2\kappa_3}\ ,$$
$$\mathbf{a} = \mathbf{q}-\boldsymbol{\Delta}+2\kappa_2\mathbf{f}_2 \quad , \quad \mathbf{b} = \mathbf{q}+\boldsymbol{\Delta}-2\kappa_3\mathbf{f}_3 \quad ,$$
$$\mathbf{c} = \mathbf{q}+\boldsymbol{\Delta}-2\varepsilon\mathbf{f}_{23} \quad , \quad \tilde{\mathbf{c}} = \mathbf{q}-\boldsymbol{\Delta}+2\varepsilon\mathbf{f}_{23} \quad .$$

Note that vectors $\mathbf{e}$ and $\mathbf{e}^*$ appeared in denominators in (2) owing to the use of the relation $2(\mathbf{e}\mathbf{a})(\mathbf{e}^*\mathbf{a}) = \mathbf{a}^2$.

As it was mentioned above, the photon-splitting amplitude obtained in the Born approximation [2, 3] for arbitrary energies and momentum transfers is rather cumbersome. It is interesting to obtain the Born amplitude from (2). In this approximation

$$(\mathbf{e}\boldsymbol{\nabla}_\mathbf{q})\,\mathrm{Im}\left(\frac{|\mathbf{q}+\boldsymbol{\Delta}|}{|\mathbf{q}-\boldsymbol{\Delta}|}\right)^{2iZ\alpha} \longrightarrow Z\alpha\left[\frac{1}{(\mathbf{e}^*,\mathbf{q}+\boldsymbol{\Delta})}-\frac{1}{(\mathbf{e}^*,\mathbf{q}-\boldsymbol{\Delta})}\right].$$

It is convenient to rewrite the quantities $\mathcal{D}_{1-3}$ in (3) as

$$\mathcal{D}_1 = \left(\mathbf{q} + \frac{\kappa_2 - \kappa_3}{\omega_1}\,\mathbf{\Delta}\right)^2 - \frac{4\omega_2\omega_3\kappa_2\kappa_3}{\omega_1^2}\mathbf{f}_{23}^2 - i0 \quad , \tag{4}$$

$$\mathcal{D}_2 = \left(\mathbf{q} - \frac{\kappa_3 + \epsilon}{\omega_3}\,\mathbf{\Delta}\right)^2 - \frac{4\omega_1\omega_2\kappa_3\epsilon}{\omega_3^2}\mathbf{f}_2^2 \quad ,$$

$$\mathcal{D}_3 = \left(\mathbf{q} + \frac{\kappa_2 - \epsilon}{\omega_2}\,\mathbf{\Delta}\right)^2 + \frac{4\omega_1\omega_3\kappa_2\epsilon}{\omega_2^2}\mathbf{f}_3^2 \quad .$$

After that we shift the variable of integration $\mathbf{q}$ in each term so that the quantities $\mathcal{D}_{1-3}$ become independent of the angle $\phi$ of the vector $\mathbf{q}$. For instance, in the terms containing $\mathcal{D}_1$ we make the substitution $\mathbf{q} \to \mathbf{q} - \frac{\kappa_2-\kappa_3}{\omega_1}\,\mathbf{\Delta}$. After passing to the variable $z = \exp(i\phi)$ we can easily take the corresponding contour integral. Taking also the integrals with respect to $|\mathbf{q}|$ and $\epsilon$, we get for the Born amplitudes

$$M_{+--} = \frac{2iZ\alpha e^3(\mathbf{f}_2 \times \mathbf{f}_3)_z}{\pi\mathbf{\Delta}^2(\mathbf{e}^*\mathbf{f}_2)(\mathbf{e}^*\mathbf{f}_3)(\mathbf{e}^*\mathbf{f}_{23})} \quad , \tag{5}$$

$$M_{+++} = \frac{2(Z\alpha)e^3\omega_1}{\pi\mathbf{\Delta}^2(\mathbf{ef}_{23})^2\omega_2\omega_3}\Bigg\{(\mathbf{e\Delta})\Bigg[1 + \frac{(\mathbf{ef}_2) + (\mathbf{ef}_3)}{(\mathbf{ef}_{23})}\ln(\frac{a_2}{a_3}) +$$

$$+\frac{(\mathbf{ef}_2)^2 + (\mathbf{ef}_3)^2}{(\mathbf{ef}_{23})^2}\left(\frac{\pi^2}{6} + \frac{1}{2}\ln^2(\frac{a_2}{a_3}) + \mathrm{Li}_2(1-a_2) + \mathrm{Li}_2(1-a_3)\right)\Bigg] +$$

$$+\frac{1}{(\mathbf{e\Delta})}\Bigg[\omega_3^2(\mathbf{ef}_3)^2\frac{a_2}{1-a_2}\left(1 + \frac{a_2\,\ln(a_2)}{1-a_2}\right) +$$

$$+\omega_2^2(\mathbf{ef}_2)^2\frac{a_3}{1-a_3}\left(1 + \frac{a_3\,\ln(a_3)}{1-a_3}\right)\Bigg] +$$

$$+\frac{2(\mathbf{ef}_2)(\mathbf{ef}_3)}{(\mathbf{ef}_{23})}\left[\omega_3\frac{a_2\,\ln(a_2)}{1-a_2} - \omega_2\frac{a_3\,\ln(a_3)}{1-a_3}\right]\Bigg\} \quad ,$$

$$M_{++-} = \frac{2(Z\alpha)e^3\omega_2}{\pi\mathbf{\Delta}^2(\mathbf{e}^*\mathbf{f}_3)^2\omega_1\omega_3}\Bigg\{(\mathbf{e}^*\mathbf{\Delta})\Bigg[1 - \frac{(\mathbf{e}^*\mathbf{f}_2) + (\mathbf{e}^*\mathbf{f}_{23})}{(\mathbf{e}^*\mathbf{f}_3)}\ln(\frac{-a_1}{a_2}) +$$

$$+\frac{(\mathbf{e}^*\mathbf{f}_2)^2 + (\mathbf{e}^*\mathbf{f}_{23})^2}{(\mathbf{e}^*\mathbf{f}_3)^2}\left(\frac{\pi^2}{6} + \frac{1}{2}\ln^2(\frac{-a_1}{a_2}) + \mathrm{Li}_2(1-a_2) + \mathrm{Li}_2(1+a_1)\right)\Bigg] +$$

$$+\frac{1}{(\mathbf{e}^*\mathbf{\Delta})}\Bigg[\omega_3^2(\mathbf{e}^*\mathbf{f}_{23})^2\frac{a_2}{1-a_2}\left(1 + \frac{a_2\,\ln(a_2)}{1-a_2}\right) -$$

$$-\omega_1^2(\mathbf{e}^*\mathbf{f}_2)^2\frac{a_1}{1+a_1}\left(1 - \frac{a_1\,\ln(-a_1)}{1+a_1}\right)\Bigg] +$$

$$+\frac{2(\mathbf{e}^*\mathbf{f}_2)(\mathbf{e}^*\mathbf{f}_{23})}{(\mathbf{e}^*\mathbf{f}_3)}\left[\omega_1\frac{a_1\,\ln(-a_1)}{1+a_1} - \omega_3\frac{a_2\,\ln(a_2)}{1-a_2}\right]\Bigg\} \quad ,$$

where

$$a_1 = \frac{\mathbf{\Delta}^2}{\omega_2\omega_3\mathbf{f}_{23}^2} \quad , \quad a_2 = \frac{\mathbf{\Delta}^2}{\omega_1\omega_2\mathbf{f}_2^2} \quad , \quad a_3 = \frac{\mathbf{\Delta}^2}{\omega_1\omega_3\mathbf{f}_3^2} \quad ,$$

$$\mathrm{Li}_2(x) = -\int\limits_0^x \frac{dt}{t}\ln(1-t) \quad .$$

It follows from (3) that $\ln(-a_1)$ should be interpreted as $\ln(-a_1+i0) = \ln(a_1) + i\pi$. Besides,

$$\mathrm{Li}_2(1+a_1) = \mathrm{Li}_2(1+a_1-i0) = \frac{\pi^2}{6} - \ln(1+a_1)[\ln(a_1)+i\pi] - \mathrm{Li}_2(-a_1)$$

The result (5) is obtained for $|\mathbf{\Delta}_\perp| \gg |\mathbf{\Delta}_z|$. One can show that it remains valid in the case $|\mathbf{\Delta}_\perp| \sim |\mathbf{\Delta}_z|$ if the expression (1) for $\mathbf{\Delta}^2$ is used in (5). Actually, in eq. (5) the difference between $\mathbf{\Delta}^2$ and $\mathbf{\Delta}_\perp^2$ is essential only in the overall factor $1/\mathbf{\Delta}^2$. For a screened Coulomb potential the amplitudes (5) should be multiplied by the atomic form factor $(1-F(\Delta^2))$. For the case of Molière potential [10] it reads

$$1 - F(\Delta^2) = \Delta^2 \sum_{i=1}^{3} \frac{\alpha_i}{\Delta^2 + \beta_i^2}\,, \tag{6}$$

where

$$\alpha_1 = 0.1 \quad , \quad \alpha_2 = 0.55 \quad , \quad \alpha_3 = 0.35 \quad , \quad \beta_i = \beta_0 b_i \quad , \tag{7}$$

$$b_1 = 6 \quad , \quad b_2 = 1.2 \quad , \quad b_3 = 0.3 \quad , \quad \beta_0 = mZ^{1/3}/121 \quad .$$

Remind, that the representation (5) is valid when $|\mathbf{k}_{2\perp}|\,, |\mathbf{k}_{3\perp}| \gg m$.

Let us consider the asymptotics of the amplitudes (2) at $|\mathbf{\Delta}_\perp| \ll |\boldsymbol{\rho}|$, where $\mathbf{\Delta}_\perp = \omega_2\mathbf{f}_2 + \omega_3\mathbf{f}_3$ and $\boldsymbol{\rho} = (\omega_2\mathbf{f}_2 - \omega_3\mathbf{f}_3)/2$. It is this region of variables which gives the main contribution to the cross section in the Weizsäcker-Williams approximation. To get this asymptotics we multiply $\mathbf{T}$ in (2) by

$$1 = \vartheta(q_0^2 - \mathbf{q}^2) + \vartheta(\mathbf{q}^2 - q_0^2) \quad ,$$

where $|\mathbf{\Delta}| \ll q_0 \ll |\boldsymbol{\rho}|$. Then, for the term in (2) proportional to $\vartheta(q_0^2 - \mathbf{q}^2)$ one can put $\mathbf{q} = 0$ and $\mathbf{\Delta} = 0$ in $\mathbf{T}$ and integrate by parts over $\mathbf{q}$. After that, using the relation $\boldsymbol{\nabla}_\mathbf{q}\vartheta(q_0^2 - \mathbf{q}^2) = -2\mathbf{q}\,\delta(q_0^2 - \mathbf{q}^2)$ one can easily take the integral over $\mathbf{q}$ since at $|\mathbf{q}| = q_0 \gg |\mathbf{\Delta}|$ one has

$$\mathrm{Im}\left(\frac{|\mathbf{q}+\mathbf{\Delta}|}{|\mathbf{q}-\mathbf{\Delta}|}\right)^{2iZ\alpha} \approx 4Z\alpha\,\frac{\mathbf{q}\mathbf{\Delta}}{\mathbf{q}^2} \quad .$$

As a result, in the region $|\mathbf{q}| < q_0$ the term proportional to $Z\alpha$ is independent of $q_0$ and the terms of next orders in $Z\alpha$ are small in the parameter $|\mathbf{\Delta}|/q_0$.

For the term proportional to $\vartheta(\mathbf{q}^2 - q_0^2)$ we get

$$\boldsymbol{\nabla}_\mathbf{q}\mathrm{Im}\left(\frac{|\mathbf{q}+\mathbf{\Delta}|}{|\mathbf{q}-\mathbf{\Delta}|}\right)^{2iZ\alpha} \approx 4Z\alpha\,\frac{\mathbf{q}^2\mathbf{\Delta} - 2\mathbf{q}(\mathbf{q}\mathbf{\Delta})}{|\mathbf{q}|^4} \quad .$$

We put $\mathbf{\Delta} = 0$ in $\mathbf{T}$ and perform the integration first over the angles of $\mathbf{q}$ and then over $|\mathbf{q}|$. As a result, the main in $q_0/|\boldsymbol{\rho}|$ contribution is independent of $q_0$ and proportional to $Z\alpha$. Taking the sum of the contributions from these two regions and performing the integration over the energy $\varepsilon$, we get

$$M_{+--} = \frac{4iN(\mathbf{e}\boldsymbol{\rho})^3}{\boldsymbol{\rho}^4}(\mathbf{\Delta}\times\boldsymbol{\rho})_z \quad , \quad N = \frac{4Z\alpha e^3\omega_2\omega_3}{\pi\omega_1\mathbf{\Delta}^2\boldsymbol{\rho}^2}\,; \tag{8}$$

$$M_{+++} = N\left[\mathbf{e}^*\mathbf{\Delta} + 2(\mathbf{e}\mathbf{\Delta})\frac{(\mathbf{e}^*\boldsymbol{\rho})^2}{\boldsymbol{\rho}^2}\left(1+\frac{\omega_2-\omega_3}{\omega_1}\ln\frac{\omega_3}{\omega_2}+\right.\right.$$

$$\left.\left.+\frac{\omega_2^2+\omega_3^2}{2\omega_1^2}(\ln^2\frac{\omega_3}{\omega_2}+\pi^2)\right)\right]$$

$$M_{++-} = N\left[\mathbf{e}\mathbf{\Delta} + 2(\mathbf{e}^*\mathbf{\Delta})\frac{(\mathbf{e}\boldsymbol{\rho})^2}{\boldsymbol{\rho}^2}\left(1+\frac{\omega_1+\omega_3}{\omega_2}(\ln\frac{\omega_3}{\omega_1}+i\pi)+\right.\right.$$

$$\left.\left.+\frac{\omega_1^2+\omega_3^2}{2\omega_2^2}(\ln^2\frac{\omega_3}{\omega_1}+2i\pi\ln\frac{\omega_3}{\omega_1})\right)\right].$$

In the small-angle approximation ($|\mathbf{f}_2|, |\mathbf{f}_3| \ll 1$) the cross section of the process reads:

$$d\sigma = \frac{\omega_1^2}{2^8\pi^5}|M|^2\,x(1-x)dx\,d\mathbf{f}_2\,d\mathbf{f}_3 \quad , \tag{9}$$

where $x = \omega_2/\omega_1$, so that $\omega_3 = \omega_1(1-x)$. In terms of the variables $\boldsymbol{\rho}$ and $\mathbf{\Delta}$ the cross section has the form

$$d\sigma = |M|^2\,\frac{d\mathbf{\Delta}\,d\boldsymbol{\rho}\,dx}{2^8\pi^5\omega_1^2\,x(1-x)} \quad , \tag{10}$$

Substituting (8) into (10) and performing the elementary integration over the angles of vectors $\mathbf{\Delta}$ and $\boldsymbol{\rho}$, we come to the expression

$$d\sigma = \frac{4Z^2\alpha^5}{\pi^2}\frac{d\rho^2\,d\Delta^2\,dx}{\rho^4\Delta^2}\,g(x) \quad , \tag{11}$$

where the function $g(x)$ for different polarizations has the form

$$g_{+++}(x) = \frac{1}{2}x(1-x)\left[1+\left(1+(2x-1)\ln\left(\frac{1-x}{x}\right)+\right.\right. \tag{12}$$

$$\left.\left.+\frac{x^2+(1-x)^2}{2}\left(\ln^2\left(\frac{1-x}{x}\right)+\pi^2\right)\right)^2\right] \quad ,$$

$$g_{++-}(x) = \frac{1}{2}x(1-x)\left[1+\left|1+(2/x-1)(\ln(1-x)+i\pi)+\right.\right.$$

$$\left.\left.+\frac{1+(1-x)^2}{2x^2}(\ln^2(1-x)+2i\pi\ln(1-x))\right|^2\right] \quad ,$$

$$g_{+--}(x) = x(1-x) \quad , \quad g_{+-+}(x) = g_{++-}(1-x) \quad .$$

Formulae (11) and (12) are in agreement with the corresponding results of [4], obtained in the Weizsäcker-Williams approximation. However, this approach does not allow to obtain the amplitudes (8) themselves. The large logarithm appears after the integration of (11)

over $\Delta^2$ from $\Delta^2_{min}$ up to $\rho^2$ where $\Delta_{min} \sim r_c^{-1}$ for the screened Coulomb potential and $\Delta_{min} \sim \rho^2/\omega_1$ for the pure Coulomb case. It is interesting to compare the contributions of different helicity amplitudes to the cross section at $\Delta \to 0$. In Fig. 1 the function $g(x)$ is shown for different helicities as well as the quantity

$$\bar{g}(x) = g_{+--}(x) + g_{+++}(x) + g_{++-}(x) + g_{+-+}(x)\,, \tag{13}$$

which corresponds to the summation over the final photon polarizations. It is seen that $\bar{g}(x)$ has a wide plateau.

The Coulomb corrections to the photon-splitting amplitude at $\Delta \to 0$ are small compared to the Born term (8). We consider the asymptotics of the Coulomb corrections at $\Delta \to 0$ in the next Section.

# 4 Coulomb corrections

To analyze the Coulomb corrections we make the further transformation of the expression (2). Let us multiply right side of (2) by

$$1 \equiv \int\limits_{-1}^{1} dy\, \delta\left(y - \frac{2\mathbf{q}\boldsymbol{\Delta}}{\mathbf{q}^2 + \boldsymbol{\Delta}^2}\right) =$$

$$(\mathbf{q}^2 + \boldsymbol{\Delta}^2) \int\limits_{-1}^{1} \frac{dy}{|y|}\, \delta((\mathbf{q} - \boldsymbol{\Delta}/y)^2 - \boldsymbol{\Delta}^2(1/y^2 - 1)) \quad ,$$

and make the substitution $\mathbf{q} \to \mathbf{q} + \boldsymbol{\Delta}/y$. After that the integral over $|\mathbf{q}|$ becomes trivial, and the integral over the angle of $\mathbf{q}$ can be easily taken by means of the residue technique. Finally, we get

$$M = \frac{4e^3 Z\alpha}{\pi\omega_1\omega_2\omega_3\boldsymbol{\Delta}^2} \int\limits_{-1}^{1} \frac{dy\ \mathrm{sign}\, y}{1-y^2} \left[\mathrm{Re}\left(\frac{1+y}{1-y}\right)^{iZ\alpha}\right] R\,; \tag{14}$$

$$R_{+--} = q^2 \int\limits_0^{\omega_2} d\varepsilon\, \frac{\kappa_2\,(\mathbf{e}^*, \kappa_2\mathbf{f}_2 - \boldsymbol{\Delta})}{(\mathbf{e}^*\mathbf{f}_3)(\mathbf{e}^*\mathbf{f}_{23})}\, \frac{\vartheta(\mathbf{r}^2 - q^2)}{(\mathbf{e}^*\mathbf{r})^2} + \begin{pmatrix}\omega_2 \leftrightarrow \omega_3\\ \mathbf{f}_2 \leftrightarrow \mathbf{f}_3\end{pmatrix} \quad ;$$

$$R_{+++} = \int\limits_0^{\omega_2} d\varepsilon \left[\frac{\omega_3\varepsilon\kappa_2}{\omega_2}\left(\frac{s}{\sqrt{s^2 - 4q^2\mathbf{u}^2}} - 1\right) \times\right.$$

$$\times \left(\frac{\omega_3}{(\mathbf{eu})} - \frac{8(\mathbf{e}^*\mathbf{f}_3)(\kappa_2^2 + \kappa_3^2)}{s - \sqrt{s^2 - 4q^2\mathbf{u}^2} - 4(\mathbf{e}^*\mathbf{r})(\mathbf{eu})}\right) +$$

$$\left. + \vartheta(q^2 - \mathbf{r}^2) \frac{(\kappa_2^2 + \kappa_3^2)\kappa_2(1 + 1/y)(\mathbf{e}^*\mathbf{f}_2)(\mathbf{e}\boldsymbol{\Delta})}{(\mathbf{ef}_{23})[\varepsilon(\mathbf{e}^*\mathbf{r})(\mathbf{ef}_{23}) - \kappa_2(1 + 1/y)(\mathbf{e}\boldsymbol{\Delta})(\mathbf{e}^*\mathbf{f}_2)]}\right] +$$

$$+ \begin{pmatrix}\omega_2 \leftrightarrow \omega_3\\ \mathbf{f}_2 \leftrightarrow \mathbf{f}_3\end{pmatrix} \quad ;$$

$$R_{++-}=\int\limits_0^{\omega_2}d\varepsilon\left[\frac{\omega_3\kappa_2\kappa_3}{\omega_1}\left(\frac{is_1}{\sqrt{4q^2\mathbf{u}_1^2-s_1^2}}-1\right)\times\right.$$

$$\times\left(\frac{\kappa_2-\varepsilon}{(\mathbf{e}^*\mathbf{u}_1)}+\frac{8(\mathbf{e}\mathbf{f}_{23})(\kappa_2^2+\varepsilon^2)}{s_1+i\sqrt{4q^2\mathbf{u}_1^2-s_1^2}-4(\mathbf{e}\mathbf{r})(\mathbf{e}^*\mathbf{u}_1)}\right)+$$

$$\left.+\vartheta(q^2-\mathbf{r}^2)\frac{(\kappa_2^2+\varepsilon^2)\kappa_2(1+1/y)(\mathbf{e}\mathbf{f}_2)(\mathbf{e}^*\mathbf{\Delta})}{(\mathbf{e}^*\mathbf{f}_3)[\kappa_3(\mathbf{e}\mathbf{r})(\mathbf{e}^*\mathbf{f}_3)-\kappa_2(1+1/y)(\mathbf{e}^*\mathbf{\Delta})(\mathbf{e}\mathbf{f}_2)]}\right]-$$

$$-\omega_2\int\limits_{-\omega_3}^{0}d\varepsilon\,\kappa_3\left[\frac{(\mathbf{e}\mathbf{\Delta})}{\omega_1(\mathbf{e}^*\mathbf{\Delta})}\left(\frac{is_1}{\sqrt{4q^2\mathbf{u}_1^2-s_1^2}}-1\right)\times\right.$$

$$\times\left(\frac{\varepsilon\kappa_3+\kappa_2^2}{(\mathbf{e}\mathbf{u}_1)}+\frac{8(\mathbf{e}^*\mathbf{f}_{23})\kappa_3(\kappa_2^2+\varepsilon^2)}{s_1-i\sqrt{4q^2\mathbf{u}_1^2-s_1^2}-4(\mathbf{e}^*\mathbf{r}_1)(\mathbf{e}\mathbf{u}_1)}\right)+$$

$$+\frac{(\mathbf{e}\mathbf{\Delta})}{\omega_3(\mathbf{e}^*\mathbf{\Delta})}\left(\frac{s_2}{\sqrt{s_2^2-4q^2\mathbf{u}_2^2}}-1\right)\times$$

$$\times\left(\frac{\kappa_2\kappa_3-\varepsilon^2}{(\mathbf{e}\mathbf{u}_2)}+\frac{8(\mathbf{e}^*\mathbf{f}_2)\kappa_3(\kappa_2^2+\varepsilon^2)}{s_2+\sqrt{s_2^2-4q^2\mathbf{u}_2^2}-4(\mathbf{e}^*\mathbf{r}_1)(\mathbf{e}\mathbf{u}_2)}\right)+$$

$$+\vartheta(\mathbf{r}_1^2-q^2)\frac{q^2(\kappa_2^2+\varepsilon^2)}{2\omega_2(\mathbf{e}^*\mathbf{r}_1)}\left(\frac{1}{\kappa_2(\mathbf{e}^*\mathbf{r}_1)(\mathbf{e}\mathbf{f}_2)-\kappa_3(1/y-1)(\mathbf{e}\mathbf{\Delta})(\mathbf{e}^*\mathbf{f}_3)}+\right.$$

$$\left.\left.+\frac{1}{\varepsilon(\mathbf{e}^*\mathbf{r}_1)(\mathbf{e}\mathbf{f}_{23})-\kappa_3(1/y-1)(\mathbf{e}\mathbf{\Delta})(\mathbf{e}^*\mathbf{f}_3)}\right)\right].$$

Here we use the following notation:

$$\mathbf{u}=\mathbf{\Delta}\left(\frac{1}{y}-1+\frac{2\kappa_2}{\omega_2}\right),\quad \mathbf{u}_1=\mathbf{\Delta}\left(\frac{1}{y}-1+\frac{2\kappa_2}{\omega_1}\right),$$

$$\mathbf{u}_2=\mathbf{\Delta}\left(\frac{1}{y}-1-\frac{2\varepsilon}{\omega_3}\right),$$

$$q^2=\mathbf{\Delta}^2(1/y^2-1),\quad \mathbf{r}=\mathbf{\Delta}(1/y-1)+2\kappa_2\mathbf{f}_2,$$

$$\mathbf{r}_1=\mathbf{\Delta}(1/y+1)-2\kappa_3\mathbf{f}_3, \tag{15}$$

$$s=\mathbf{u}^2+q^2+\frac{4\omega_1\omega_3\kappa_2\varepsilon}{\omega_2^2}\mathbf{f}_3^2,\ s_1=\mathbf{u}_1^2+q^2-\frac{4\omega_2\omega_3\kappa_2\kappa_3}{\omega_1^2}\mathbf{f}_{23}^2-i0,$$

$$s_2=\mathbf{u}_2^2+q^2-\frac{4\omega_1\omega_2\kappa_3\varepsilon}{\omega_3^2}\mathbf{f}_2^2.$$

Since the function $R$ in (14) is independent of the parameter $Z\alpha$ the Coulomb corrections $M^{(c)}$ can be obtained from (14) by the substitution

$$\mathrm{Re}\left(\frac{1+y}{1-y}\right)^{iZ\alpha}\to\mathrm{Re}\left(\frac{1+y}{1-y}\right)^{iZ\alpha}-1$$

The asymptotics of $M^{(c)}$ at $\Delta \to 0$ depends on the photon helicities. The most simple way to get this asymptotics is to start directly from (2). For $M^{(c)}_{+--}$ the main contribution is determined by the region $q \sim \rho \gg \Delta$ (remind that $\boldsymbol{\rho} = (\omega_2 \mathbf{f}_2 - \omega_3 \mathbf{f}_3)/2$), while for $M^{(c)}_{+++}$ and $M^{(c)}_{++-}$ it comes from the region $q \sim \Delta \ll \rho$. After the corresponding expansion and integration over the energy we get at $\Delta \to 0$

$$M^{(c)}_{+--} = -\frac{2e^3 (Z\alpha)^3 \omega_2 \omega_3 \, (\mathbf{e}^* \boldsymbol{\Delta})}{\pi \omega_1 (\mathbf{e}^* \boldsymbol{\rho})^4} \ln^2 \frac{\rho}{\Delta} \quad ; \tag{16}$$

$$M^{(c)}_{+++} = -\frac{i e^3 Z\alpha \omega_2 \omega_3}{2\pi \omega_1 \rho^2 (\mathbf{e}\boldsymbol{\rho})(\mathbf{e}^* \boldsymbol{\Delta})} \times$$

$$\times \int \frac{d\mathbf{q}}{(\mathbf{e}, \mathbf{q} - \boldsymbol{\Delta})} \left[ \mathrm{Re} \left( \frac{|\mathbf{q} + \boldsymbol{\Delta}|}{|\mathbf{q} - \boldsymbol{\Delta}|} \right)^{2iZ\alpha} - 1 \right] \mathrm{sign}[(\mathbf{q} - \boldsymbol{\Delta}) \times \boldsymbol{\rho}]_z \quad ;$$

$$M^{(c)}_{++-} = -\frac{e^3 Z\alpha \omega_2^2 \omega_3}{2\pi^2 \omega_1^2 \rho^2 (\mathbf{e}^* \boldsymbol{\rho})(\mathbf{e}\boldsymbol{\Delta})} \times$$

$$\times \int \frac{d\mathbf{q}}{(\mathbf{e}^*, \mathbf{q} - \boldsymbol{\Delta})} \left[ \mathrm{Re} \left( \frac{|\mathbf{q} + \boldsymbol{\Delta}|}{|\mathbf{q} - \boldsymbol{\Delta}|} \right)^{2iZ\alpha} - 1 \right] \times$$

$$\times \left[ \ln \frac{|\mathbf{q} - \boldsymbol{\Delta}|}{\Delta} + i \mathrm{arg} \frac{\mathbf{e}(\mathbf{q} - \boldsymbol{\Delta})}{\mathbf{e}\boldsymbol{\rho}} \right] .$$

It follows from (16) that in this limiting case the Coulomb correction $M^{(c)}_{+--}$ is small, while $M^{(c)}_{+++}$ and $M^{(c)}_{++-}$ depend only on the direction of vector $\boldsymbol{\Delta}$, but not on its module (it becomes obvious after the substitution $\mathbf{q} \to \mathbf{q}\Delta$). We discuss the role of Coulomb corrections in the next Section.

# 5 Cross section

As it was suggested in [11], to overcome the problems of background in the measurement of photon splitting one has to register the events with $|\mathbf{f}_{2,3}| \geq f_0$ where $f_0 \ll 1$ is determined by the experimental conditions. Let us consider the cross section integrated over $\mathbf{f}_3$ for $|\mathbf{f}_3| > f_0$. It is interesting to compare the exact ( in $Z\alpha$ ) cross section $d\sigma/dx\, d\mathbf{f}_2$ with that obtained in the Born approximation ($d\sigma_B/dx\, d\mathbf{f}_2$) and also with the cross section in the Weizsäcker-Williams approximation ($d\sigma_W/dx\, d\mathbf{f}_2$). Remind that $d\sigma_W/dx\, d\mathbf{f}_2$ is in fact the Born cross section calculated within logarithmic accuracy. Large logarithm corresponds to the contribution of the region $\Delta \ll \rho = |\omega_2 \mathbf{f}_2 - \omega_3 \mathbf{f}_3)/2|$, where $f_3 \approx x f_2/(1-x)$. Taking the integral over $\Delta^2$ in eq. (11) from $\Delta^2_{min}$ up to $\Delta^2_{eff}$, where (see [4])

$$\Delta^2_{min} = \Delta^2_z = (\omega_1 f_2^2 x/2(1-x))^2 \, , \; \Delta^2_{eff} = \rho^2 = (\omega_1 x f_2)^2 \, ,$$

and summing over the final photon polarizations we get for a pure Coulomb potential

$$\frac{d\sigma_W}{dx\, d\mathbf{f}_2} = \frac{8Z^2\alpha^5}{\pi^3 \omega_1^2} \frac{\bar{g}(x)}{x^2 f_2^4} \ln \left( \frac{2(1-x)}{f_2} \right) \vartheta(\frac{x}{1-x} f_2 - f_0) \, . \tag{17}$$

For the case of a screened Coulomb potential the approximate cross section is

$$\frac{d\sigma_W}{dx\,d\mathbf{f}_2} = \frac{4Z^2\alpha^5}{\pi^3\omega_1^2}\,\frac{\bar{g}(x)}{x^2 f_2^4}\left[2\ln\left(\frac{\omega_1 x f_2}{\beta_0}\right)+\gamma\right]\vartheta(\frac{x}{1-x}f_2 - f_0)\,. \tag{18}$$

The function $\gamma$ in eq. (18) is

$$\gamma = 1 - \sum_{i=1}^{3}\alpha_i^2(\ln a_i + 1) - 2\sum_{i>j}\alpha_i\alpha_j\frac{a_i\ln a_i - a_j\ln a_j}{a_i - a_j}\,, \tag{19}$$

$$a_i = b_i^2 + \Delta_{min}^2/\beta_0^2$$

and the coefficients $\alpha_i$, $b_i$ and $\beta_0$ are defined in eq. (7). If $\Delta_{min}^2/\beta_0^2 \gg 1$ then $\gamma = -\ln(\Delta_{min}^2/\beta_0^2)$ and eq. (18) turns to eq. (17). If $\Delta_{min}^2/\beta_0^2 \ll 1$ then $\gamma = -0.158$.

For the case of a pure Coulomb potential the dependence of $\sigma_0^{-1}d\sigma/dxd\mathbf{f}_2$ on $f_2/f_0$ is shown in Figs. 2-4 for $f_0 = 10^{-3}$, $Z = 92$ and different values of $x$,

$$\sigma_0 = \frac{4Z^2\alpha^5}{\pi^3\omega_1^2 f_0^4} \quad .$$

In these figures the solid curves represent the exact cross sections, the dashed ones are Born results ($d\sigma_B/dx\,d\mathbf{f}_2$) and the dash-dotted are obtained in the Weizsäcker-Williams approximation. At $x = 0.7$ (Fig. 2) the difference between $d\sigma_B/dx\,d\mathbf{f}_2$ and $d\sigma_W/dx\,d\mathbf{f}_2$ is small. At $x = 0.3$ (Fig. 3) $d\sigma_B/dx\,d\mathbf{f}_2$ differs noticeably from $d\sigma_W/dx\,d\mathbf{f}_2$. Note that within a good accuracy the cross section $d\sigma_B/dx$ at $x = 0.3$ agrees with that obtained from eq. (17) after the integration over $\mathbf{f}_2$. It should be so, since $d\sigma/dx$ is invariant with respect to the substitution $x \to 1-x$ and at $x = 0.7$, as we pointed out above, the approximate result (17) is in accordance with the exact one. At $x = 0.5$ a big difference between $d\sigma_B/dx\,d\mathbf{f}_2$ and $d\sigma_W/dx\,d\mathbf{f}_2$ (see Fig. 4) in the region $f_2 \sim f_0$ can be explained as follows. The large logarithm appears as a result of integration with respect to $\mathbf{f}_3$ over the range $|(1-x)\mathbf{f}_3 + x\mathbf{f}_2| \ll xf_2$. After the integration over the azimuth angle $\varphi$ between vectors $\mathbf{f}_2$ and $-\mathbf{f}_3$ we should integrate over $f_3$ from $f_0$ up to $xf_2/(1-x)$ and from $xf_2/(1-x)$ to infinity. If $xf_2/(1-x) \approx f_0$ then the contribution of the first region vanishes and the cross section becomes approximately two times smaller (in accordance with Fig. 4). In all cases the exact cross section at $Z\alpha \sim 1$ is noticeably smaller than the Born one. The magnitude of this effect depends on kinematics. For instance, at $x = 0.3$ (Fig. 3) and $f_2 < f_0(1-x)/x$ when $\Delta \sim \rho$ the exact cross section is several times smaller than the Born one, while for $f_2 > f_0(1-x)/x$ the difference of these cross sections is about 15%. For $x = 0.5$ and 0.7 (Figs. 3,4) this difference is about 20% and almost independent of $f_2/f_0$. All indicated relations between cross sections take place also when screening is taken into account. Emphasize that at $\Delta \sim \rho$ and $Z\alpha \sim 1$ the exact cross section differential over all variables ($d\sigma/dx\,d\mathbf{f}_2 d\mathbf{f}_3$) is much smaller than the Born one. In Fig. 5 this differential cross section is shown for the case of a screened Coulomb potential. The peak for azimuth angle $\phi = \pi$ corresponds to small $\mathbf{\Delta}$. There is a narrow notch at $f_3 = xf_2/(1-x)$ which corresponds to the condition $\mathbf{\Delta}_\perp = 0$. The width $\delta f_3$ of the notch is about $\max(\Delta_z/\omega_3, \beta_0/\omega_3)$. For the parameters used in Fig. 5, $\delta f_3$ is about $10^{-4}$.

Let us discuss now the cross section $d\sigma/dx$. In the Weizsäcker-Williams approximation for a pure Coulomb potential the cross section $d\sigma_W/dx$ obtained from (17) is

$$\frac{d\sigma_W}{dx} = \pi f_0^2\, \sigma_0 \bar{g}(x) \left[ \frac{\vartheta(x-1/2)}{x^2} \left( 2\ln\frac{2(1-x)}{f_0} - 1 \right) + \right. \tag{20}$$

$$\left. + (x \leftrightarrow 1-x) \right] .$$

If $\omega_1 f_0^2/(1-x) \ll \beta_0$, then the corresponding cross section in a screened potential has the form

$$\frac{d\sigma_W}{dx} = \pi f_0^2\, \sigma_0 \bar{g}(x) \left[ \frac{\vartheta(x-1/2)}{x^2} \left( 2\ln\frac{\omega_1 x f_0}{\beta_0} + 0.842 \right) + \right. \tag{21}$$

$$\left. + (x \leftrightarrow 1-x) \right] .$$

The inequality $\Delta \ll \rho$ which provides the applicability of the Weizsäcker-Williams approximation corresponds to a small angle $\varphi$ between the vectors $\mathbf{f}_2$ and $-\mathbf{f}_3$ ( when the vectors $\mathbf{f}_2$ and $\mathbf{f}_3$ have almost opposite directions). So, it is interesting to consider the quantity $d\sigma_B(\varphi_{max})/dx$ which is the Born cross section integrated over the angle $\varphi$ from $-\varphi_{max}$ to $\varphi_{max}$. In the case of a pure Coulomb potential the dependence of $(\pi f_0^2 \sigma_0)^{-1} d\sigma_B(\varphi_{max})/dx$ on $\varphi_{max}$ is shown in Fig. 6 for different $x$ and $f_0 = 10^{-3}$. One can see that the cross section is saturated at relatively large $\varphi_{max}$. The same conclusion is valid for the case of a screened Coulomb potential.

Let us represent the exact cross section as a sum $d\sigma/dx = d\sigma_B/dx + d\sigma_C/dx$. As it was mentioned above, the region of small momentum transfers $\Delta$ is not important for the Coulomb corrections $d\sigma_C/dx$. Therefore, one can neglect the effects of screening in the calculation of $d\sigma_C/dx$. The quantity $F = (\pi f_0^2 \sigma_0)^{-1}\, d\sigma_C/dx$ is independent of $f_0$ and $\omega_1$ and is the function of $Z\alpha$ and $x$. The dependence of $F$ on $x$ for different $Z$ is shown in Fig. 7. On can see that the Coulomb corrections diminish the cross section of the process. To realize the magnitude of this effect we plot in Fig. 8 the cross sections $d\sigma/dx$, $d\sigma_B/dx$ and $d\sigma_W/dx$ for $Z = 83$ and $f_0 = 10^{-3}$. It is seen that the Coulomb corrections are important. This is the consequence of the fact that at $Z\alpha \sim 1$ the constant added to the logarithm, i.e. the quantity $x^2\, F/\bar{g}(x)$, is large enough in a wide range of $x$. Although this quantity is independent of $f_0$ and $\omega_1$, the relative contribution of the Coulomb corrections to the exact cross section depends on these parameters since the large logarithm contains them.

Due to the gauge invariance the cross section $d\sigma/dx$ should be equal to zero at $x = 1$ if the electron mass is not neglected. This is not the case for massless particles as it has been noted in [12]. That is why the cross section $d\sigma/dx$ calculated in zero-mass limit does not vanish at $x \to 1$ (see Fig. 8) . When $x \to 1$ the main contribution to the cross section comes from the range of angles $f_3 \sim f_2/\sqrt{1-x}$ and $f_2 \sim f_0$ , $\Delta \approx \omega_2 f_2$, where the Weizsäcker-Williams approximation is not applicable. Since $f_3 \ll 1$, the relation $1 - x \gg f_0^2$ should be fulfilled. Besides, the condition $k_{3,\perp} \gg m$ means that $(1-x)\omega_1\, f_3 \sim \sqrt{1-x}\omega_1\, f_0 \gg m$ or $1 - x \gg (m/\omega_1 f_0)^2$.

If we represent the amplitude $M$ of the process as a sum of Born amplitude $M_B$ and Coulomb corrections $M_C$, then $|M|^2 = |M_B|^2 + 2\,\mathrm{Re}(M_B^* M_C) + |M_C|^2$. Taking into account in $M_C$ only the lowest in $Z\alpha$ term (proportional to $(Z\alpha)^3$), we get $d\sigma_C^{(1)}/(Z\alpha)^4 = c_1 + c_2(Z\alpha)^2$ , where $c_1$ and $c_2$ are independent of $Z\alpha$ and $c_2 > 0$ . The dependence of $(Z\alpha)^{-2}(\pi f_0^2 \sigma_0)^{-1}\, d\sigma_C/dx$ on $Z\alpha$ is shown in Fig. 9 for different $x$. One can see that starting from $Z \sim 30$ the contribution of the next order Coulomb corrections essentially modifies the behavior of $d\sigma_C$.

Thus, the Coulomb corrections are very important for the adequate description of high-energy photon splitting and must be taken into account at the comparison of theory and experiment.

We are grateful to V.S. Fadin and E.A. Kuraev for useful discussions.

# References

[1] Report given at the international conference "Photon-97", Egmond-aan-Zee, Holland.

[2] Y.Shima, Phys.Rev. **142**, 944 (1966).

[3] V.Costantini, B.De Tollis and G.Pistoni, Nuovo Cimento **A 2**, 733 (1971).

[4] V.N.Baier, V.M.Katkov, E.A.Kuraev and V.S.Fadin, Phys.Lett. **B 49**, 385 (1974).

[5] A.M.Johannessen, K.J.Mork and I.Overbo, Phys.Rev. **D 22**, 1051 (1980).

[6] H.-D.Steinhofer, Z.Phys. **C 18**, 139 (1983).

[7] R.N. Lee, A.I. Milstein, V.M. Strakhovenko, Preprint Budker INP 97-35, Novosibirsk 1997, hep-ph/9704230.

[8] A.I.Milstein and V.M.Strakhovenko, Phys. Lett **A 95**, 135 (1983); Sov. Phys. JETP **58** 8 (1983).

[9] R.N.Lee and A.I.Milstein, Phys. Lett. **A 198**, 217 (1995); Sov. Phys. JETP **80** 777 (1995).

[10] G.Z.Molière, Naturforsch. **2a**, 133 (1947).

[11] A.I.Milstein and B.B.Wojtsekhowski, It is possible to observe photon splitting in a strong Coulomb field, Preprint INP 91-14, Novosibirsk 1991.

[12] E.A.Kuraev, Thesis, p.203, Budker INP, Novosibirsk (1984).

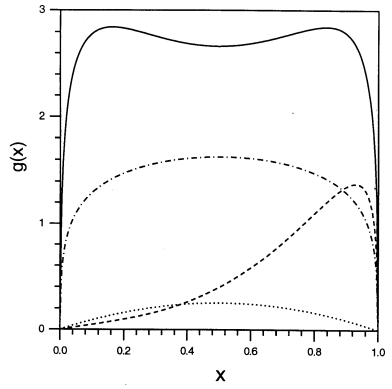


Figure 1: Function $g(x)$ from eq. (12) for different polarizations: $g_{+--}(x)$ (dotted curve),$g_{++-}(x)$ (dashed curve),$g_{+++}(x)$ (dash-dotted curve), and $\bar{g}(x)$ (solid curve), eq. (13).

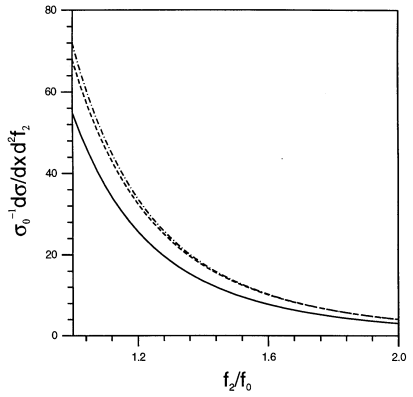


Figure 2: $\sigma_0^{-1} d\sigma/dx d\mathbf{f}_2$ versus $f_2/f_0$ for a pure Coulomb potential, $f_0 = 10^{-3}$, $x = 0.7$, $Z = 92$, $\sigma_0$ is given in the text. The dash-dotted curve corresponds to the Weizsäcker-Williams approximation, the dashed curve gives the Born approximation, the solid curve is the exact result.

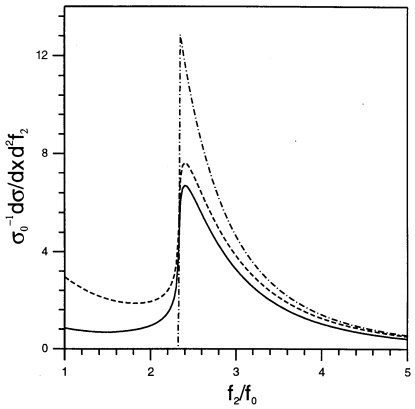


Figure 3: Same as Fig. 4 but for $x = 0.3$ .

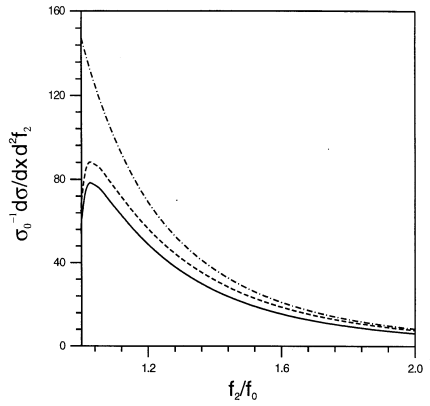


Figure 4: Same as Fig. 4 but for $x = 0.5$ .

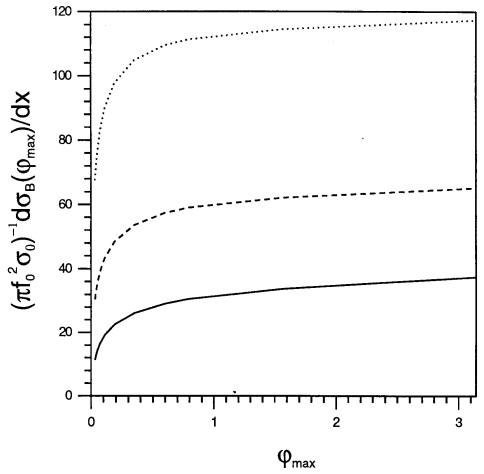


Figure 5: Differential cross section $d\sigma/dx d\mathbf{f}_2 d\mathbf{f}_3$ versus $f_3$ in a screened Coulomb potential for different azimuth angle $\phi$ between vectors $\mathbf{f}_2$ and $\mathbf{f}_3$; $Z = 83$, $x = 0.7$, $\omega_1 = 1$GeV, $f_2 = 5$mrad. The dashed curve (Born approximation) and the solid curve (exact cross section) correspond to $\phi = \pi$. The dash-dotted curve (Born approximation) and the dotted curve (exact cross section) correspond to $\phi = \pi/2$.

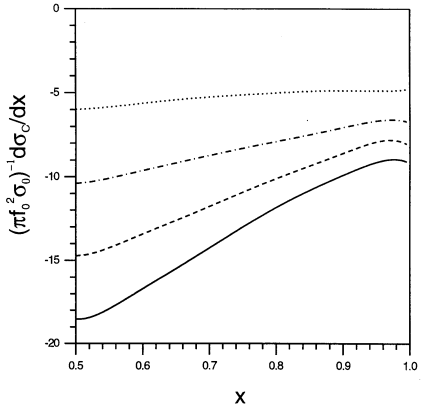


Figure 6: The dependence of $(\pi f_0^2 \sigma_0)^{-1} d\sigma(\varphi_{max})/dx$ on $\varphi_{max}$ for a pure Coulomb potential at different $x$: $x = 0.5$ (dotted curve), $x = 0.7$ (dashed curve), and $x = 0.9$ (solid curve); $f_0 = 10^{-3}$.

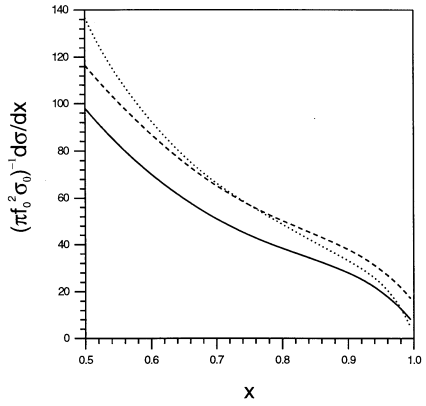


Figure 7: The dependence of $(\pi f_0^2\sigma_0)^{-1}d\sigma_C/dx$ on $x$ for Z=32 (dotted curve), 47 (dash-dotted curve), 64 (dashed curve) and 83 (solid curve).

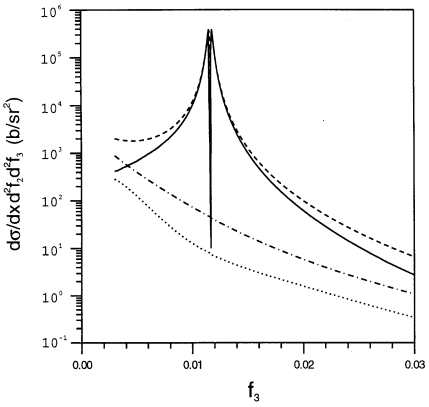


Figure 8: The dependence of $(\pi f_0^2\sigma_0)^{-1}d\sigma/dx$ on $x$ for Z=83, $f_0 = 10^{-3}$. The dotted curve corresponds to the Weizsäcker-Williams approximation, the dashed curve gives the Born approximation and the solid one shows the result exact in $Z\alpha$.

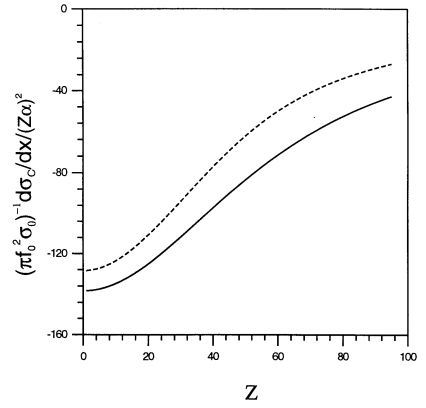


Figure 9: The dependence of $(\pi f_0^2\sigma_0)^{-1}d\sigma_C/dx/(Z\alpha)^2$ on $Z$ for x=0.5 (solid curve) and x=0.8 (dashed curve).